ELSEVIER

Journal of Nuclear Materials 283–287 (2000) 1171–1176

journal of nuclear materials

www.elsevier.nl/locate/jnucmat

Hydrodynamic effects of eroded materials of plasma-facing component during a Tokamak disruption

A. Hassanein *,[1], I. Konkashbaev

Argonne National Laboratory, Bldg 362, 9700 South Cass Avenue, Argonne, IL 60439, USA

Abstract

Loss of plasma confinement causes surface and structural damage to plasma-facing materials (PFMs) and remains a major obstacle for tokamak reactors. The deposited plasma energy results in surface erosion and structural failure. The surface erosion consists of vaporization, spallation, and liquid splatter of metallic materials, while the structural damage includes large temperature increases in structural materials and at the interfaces between surface coatings and structural members. Comprehensive models (contained in the HEIGHTS computer simulation package) are being used self-consistently to evaluate material damage. Splashing mechanisms occur as a result of volume bubble boiling and liquid hydrodynamic instabilities and brittle destruction mechanisms of nonmelting materials. The effect of macroscopic erosion on total mass losses and lifetime is evaluated. The macroscopic erosion products may further protect PFMs from severe erosion (via the droplet-shielding effect) in a manner similar to that of the vapor-shielding concept.

1. Introduction

Erosion and structural damage due to loss of plasma confinement in a tokamak remain major obstacles to a successful reactor concept. The extent of such damage depends on the detailed physics of the disrupting plasma, the physics of plasma/material interactions, and the design configuration of the plasma-facing components (PFCs). Plasma instabilities can cause both surface and bulk damage to surface and structural materials [1]. Surface damage includes high erosion losses from surface vaporization, spallation, and melt-layer erosion. Bulk damage includes large temperature increases that can cause high thermal stresses, possible melting, and material fatigue and failure.

The comprehensive HEIGHTS package has been developed and being used to study in detail the various effects of sudden high-energy deposition of different sources on target materials [2]. The present work focuses mainly on modeling the behavior and macroscopic erosion of metallic surfaces and brittle-destruction erosion of carbon-based materials (CBMs). Macroscopic erosion products may further shield the target surface and reduce total erosion losses. Lifetime estimates of plasma-facing materials (PFMs) due to disruption erosion in a tokamak device are presented. Loss of vapor-cloud confinement and vapor removal due to MHD effects and damage to nearby surfaces due to intensive vapor radiation can significantly increase erosion losses.

2. Erosion mechanisms

The vapor cloud that quickly develops above the surface material during a disruption, if well confined, will shield the original surface from the incoming energy flux and significantly reduce the heat load onto the exposed plate surface [1,3]. This vapor-shielding layer completely absorbs the incoming particle flux therefore, heating it to temperatures of up to several tens of eV. At such temperatures, the vapor plasma radiation becomes comparable with the incoming power. Because of absorption by a colder, denser, and correspondingly more optically

* Corresponding author. Tel.: +1-630 252 5889; fax: +1-630 252 5287.

E-mail address: hassanein@anl.gov (A. Hassanein).

[1] Permanent address: Troitsk Institute for Innovation and Fusion Research, Russian Federation.

0022-3115/00/$ - see front matter
PII: S0022-3115(00)00142-2

thick vapor plasma near the exposed surface, radiation power to the plate surface is significantly decreased.

2.1. Surface vaporization

The detailed vapor motion above the exposed surface is calculated by solving the vapor MHD equations for conservation of mass, momentum, and energy under the influence of a strong magnetic field [2]. A significant part of the incident plasma kinetic energy is quickly transformed into vapor-generated photon radiation. The net heat flux reaching the surface will then determine the net erosion from surface vaporization and erosion from liquid splashing and brittle destruction.

Fig. 1 shows a typical time evolution of a tungsten-surface temperature, melt-layer thickness, and vaporization losses during a disruption for an incident plasma energy of 10 MJ/m^2 deposited in a disruption time of 1 ms, as predicted by the HEIGHTS package [2]. An initial magnetic field strength of 5 T with an incident angle of 2° is assumed in this analysis. The sharp initial rise in surface temperature is due to the direct energy deposition of incident plasma particles at the material surface. The subsequent decrease in surface temperature is caused by the shielding effect of the eroded material accumulated above the target surface. HEIGHTS calculations predict that radiation power W_s onto the target surface is <10% of the original incident power [3].

2.2. Macroscopic liquid erosion and brittle destruction

Net radiation power reaching the target surface will result in surface vaporization and surface ablation, i.e., mass loss in the form of macroscopic particles. Modeling predictions have shown that surface vaporization losses of metallic materials are small (only a few micrometers deep; see Fig. 1) due to the self-shielding effect. However, for a liquid metal surface, ablation was predicted theoretically to be in the form of macroscopic metal droplets due to splashing of the molten layer [4]. Mass losses in simulation experiments are found to be in the form of liquid metal droplets with average sizes of a few tens of micrometers leaving the target surface with velocities $U \approx 10$–50 m/s [5–7]. Such ablation occurs as a result of splashing of the liquid layer mainly due to boiling and explosion of gas bubbles in the liquid, absorption of plasma momentum, and hydrodynamic instabilities developed in the liquid layer from various forces [8].

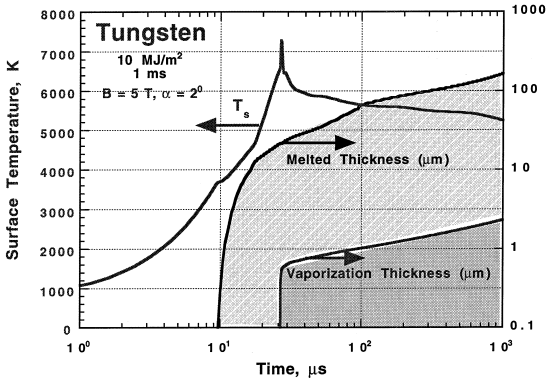

Fig. 1. Time evolution of tungsten surface temperature, melt layer, and vaporization thickness during plasma instabilities.

Hydrodynamic instabilities can occur if the vapor plasma is not well confined by the magnetic field and vapor flow occurs along the target surface [9]. Volume bubble boiling [4,10] usually occurs from overheating of the liquid metal above the vaporization temperature. Therefore, splashing erosion energy is roughly equal to the sum of the thermal energy, heat of fusion, and kinetic energy of the droplets. The kinetic energy of the splashed droplets is determined from the surface tension of the liquid metal.

Non-metallic materials such as graphite and CBMs have also shown large erosion losses significantly exceeding that from surface vaporization [11–13]. This macroscopic erosion depends on three main parameters: net power flux to the surface, exposure time, and threshold energy required for brittle destruction. The required energy for brittle destruction of graphite is estimated to be ≈10 kJ/g, or 20 kJ/cm^3 [13]. As an example, assuming a net power flux to the material surface during the disruption of ≈300 kW/cm^2, the deposited energy for a time of 1 ms is ≈0.3 kJ/cm^2, which then results in net erosion of ≈150 μm per disruption. This value is significantly higher than that predicted from pure surface vaporization of ≈10 μm per disruption for CBMs [14]. Therefore, more-relevant experimental data and more-detailed modeling are needed to evaluate the erosion of CBMs.

To correctly predict macroscopic erosion due to ablation, a four-moving-boundaries problem is solved in the HEIGHTS package. The front of the vapor cloud is one moving boundary determined by solving vapor hydrodynamic equations. The second moving boundary due to surface vaporization of the target is calculated from target thermodynamics. The third moving boundary is due to the melt-splashing front. Finally, the fourth moving boundary is at the liquid/solid interface, which determines the new thickness of the melt layer. The SPLASH code, part of the HEIGHTS package, calculates mass losses using a splashing/destruction-wave concept from each erosion-causing mechanism [15].

3. Macroscopic or droplet-shielding concept

The ejected macroscopic particles from CBMs or metallic droplets (both referred as MP) will also form a

cloud within the vapor cloud near the target surface. Photon radiation power then be absorbed by the target surface and by the mixture of both vapor and droplets cloud above the surface. This will also result in surface vaporization of droplets. This has the effect of reducing photon radiation power to the target surface. Such screening is called 'droplet shielding' in analogy to the vapor shielding effect [1]. Fig. 2 is a schematic illustration of the droplet or macroscopic shielding concept during loss of plasma confinement.

Consideration of droplet shielding effect will further be explored using an analytical solution to provide insight to the role of the various physical and material processes controlling overall erosion mechanisms. The analytical solution is complementary to the ongoing detailed numerical models to study vapor and droplet shielding phenomena that are currently being implemented in the HEIGHTS package.

For the analytical solution, we consider particles with an average radius R_d and velocity U in the normal direction to target surface. Heat conduction from the vapor to MP is very small and is neglected. Because MP will absorb some of the photon radiation, only part of this radiation, W_s, achieves the plate surface, $W_s < W_0$, where W_0 is the total photon radiation flux toward the target surface. This part of the radiation reaching the surface is also spent in surface vaporization and ablation, i.e., MP formation. Because vaporization energy q_v is much higher than the energy for ablation q_d, surface radiation power is mostly spent in MP formation. The

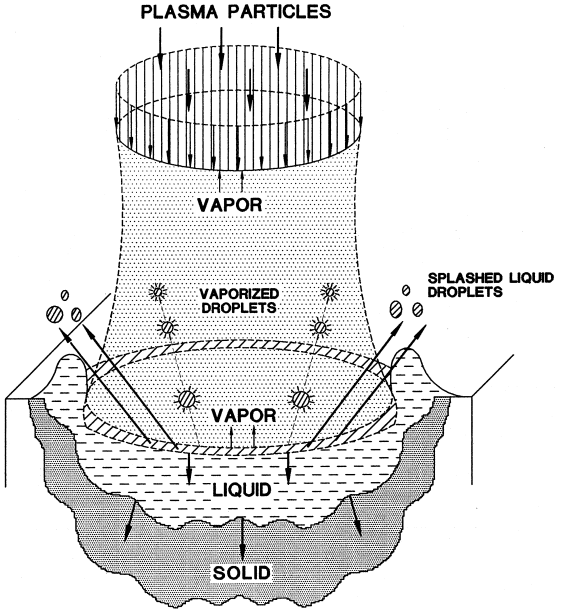

Fig. 2. Schematic illustration of droplet and macroscopic shielding concept during plasma/material interaction following plasma instabilities.

number of MP per unit volume, i.e., density of MP n_{d0}, with an average radius R_{d0} leaving the surface with a velocity U_{d0} is given by

$$n_{d0} = \frac{W_s}{q_d V_{d0} U_{d0}}, \quad \text{where } V_{d0} = \frac{4}{3}\pi R_{d0}^3, \tag{1}$$

$$q_d = q_{th} + \Delta q, \quad q_{th} \approx c_v T_s, \quad \text{and} \quad \Delta q = q_s + q_k, \tag{2}$$

where q_d is destruction energy (for liquid splashing or brittle destruction), q_s the energy required to separate MP from the surface, q_k the kinetic energy of MP, c_v the specific heat, and T_v is the vaporization temperature, i.e., the saturation temperature at the corresponding vapor pressure above the target surface. Both q_k and q_s are calculated to be very small compared to q_{th} and will be ignored in the analytical solution.

Because ejected MP from target surface will absorb photon radiation, the equation for the spatial variation of the radiation power W is

$$\frac{dW}{dx} = -\frac{W}{l_v}, \quad l_v = \frac{1}{n_d \sigma}, \quad \sigma = \zeta \pi R_d^2, \tag{3}$$

where ζ is absorption coefficient, $\zeta \leqslant 1$, and l_v is the mean path length of photons. The absorbed energy is mainly spent in the vaporization of MP

$$U \frac{dV_d}{dx} = -\frac{W}{q_v}\sigma. \tag{4}$$

Eqs. (3) and (4) have a solution with the ratio between W_s and W_0 given by

$$\frac{W_s}{W_0} = \frac{1}{1+\lambda}, \quad \text{and} \quad \lambda = \frac{q_v}{q_d} \tag{5}$$

Therefore, radiation power to the surface decreases by a factor $(1+\lambda)^{-1}$ due to droplet shielding. For a lithium target, $\lambda = q_v/q_s \approx 3.66$, and $W_s/W_0 = 0.2$, i.e., only $\approx$20% of the incoming radiation energy is deposited directly on the target surface. It is interesting to note that the ratio W_s/W_0 does not depend on size or velocity distributions of the ejected MP, but only on energies of destruction q_d and vaporization q_v.

The distance L at which MP are entirely vaporized, i.e., when $R_d = 0$, can then given from the solution of above equations as

$$\frac{L}{R_{d0}} = U \frac{q_v}{W_0} \frac{4}{\zeta} F, \quad F = \frac{v_0}{u_0}, \quad u_0 = \sqrt[3]{\frac{\lambda}{1+\lambda}}, \tag{6}$$

$$v_0 = \frac{1}{3} \ln \frac{\sqrt{1+u_0+u_0^2}}{1-u_0} + \frac{1}{\sqrt{3}} \operatorname{arctg} \frac{u_0\sqrt{3}}{2+u_0}. \tag{7}$$

Usually, $10 > \lambda > 1$; thus $u_0 \approx 1$ and $1 < F < 20$. For example, for a liquid lithium target, $F(\lambda = 3.7) = 7.85$ and for $\zeta \approx 1$;

$$\frac{L}{R_{d0}} \approx 7.7 \frac{U(\mathrm{m/s})}{W_0(\mathrm{MW/cm^2})}. \quad (8)$$

The radiation power to a divertor surface during a plasma disruption is calculated to be $W_0 \approx 0.8$ MW/cm^2 for a lithium target [1]. For lithium droplets having $U \approx 10$ m/s and $R_{d0} \approx 10$ μm, they will be vaporized at a distance $L \approx 100\ R_{d0}$, i.e., $L < 1$ cm.

It is also important to take into account that some MP are emitted near the target edge with bandwidth $\Delta y \leqslant L$ and therefore will not be fully vaporized. A fraction of MP mass $\approx 2L/L_d$, where L_d is target width, leaves the vapor cloud without being vaporized and is redeposited on nearby components. Nevertheless, total erosion mass loss can increase by the ratio $\approx 2L/L_d$ $(1 + \lambda)$. This could be particularly significant in simulation experiments where the exposed target is of the order of MP vaporization length.

4. Total mass losses and lifetime of PFMs

Numerical calculations have shown that there are several stages of plasma flow interaction with target materials. Due to the initial high power load, the material surface is heated to a temperature sufficient for intense vaporization. The shielding layer then forms in time duration, τ_{vapor}, of ≈10–20 μs. Target surface temperature decreases due to reduction of radiation power at the surface, and only after some time, τ_{cond}, the surface temperature rises again and reaches a 'vaporization temperature' sufficient to start volume-bubble boiling or brittle destruction. Then, after time $\geqslant \tau_{delay} = \tau_{vapor} + \tau_{cond}$, the process has a quasistationary character in which the radiation power to the surface is spent for vaporization, droplet emission, and heat conduction into the target bulk. The τ_{cond} depends on the incoming radiation power to the surface and material thermodynamic properties. The delay time τ_{delay} is calculated for the candidate materials Be, C, and W to be ≈70, 150, and 300 μs, respectively.

The time dependence of both melting and splashing fronts of a tungsten target for a net radiation power to the surface of 100 kW/cm^2 is shown in Fig. 3. The melting front moves initially with time as $t^{-1/2}$ for time $t < \tau_{delay}$. When splashing starts at temperature $T = T_v$, and liquid droplets are removed, the distance between the splashing surface and the melting front remains constant. This means that all incoming radiation power to surface is spent for splashing.

Fig. 4 shows the time dependence of tungsten splashing-erosion depth for various radiation powers on a tungsten surface without droplet shielding effect. The delay time required to heat the surface to a temperature above the splashing condition depends on incoming radiation power S_{rad} as S^{-2}. It can be seen that decreasing S_{rad} from 0.3 to 0.1 MW/cm^2 increases the delay time from 60 to 600 μs, respectively. This finding has two significant implications. First is that the level of radiation power substantially increases the MP erosion rate (from 100 μm at 0.1 MW/cm^2 to 900 μm at 0.3 MW/cm^2, without droplet shielding). Second, it can explain why in some simulation experiments that significant splashing, particularly with high-Z targets such as tungsten, was not seen because of the short time duration of these simulation devices which is less than the time delay required for S_{rad} associated with such experiments. Therefore, for adequate simulation of the effect of reactor plasma instabilities on erosion lifetime, facilities with long time duration >300 μs are needed. In the VIKA disruption simulation facility [16], it was shown that for different target materials, significant erosion starts after some delay time similar to that predicted above.

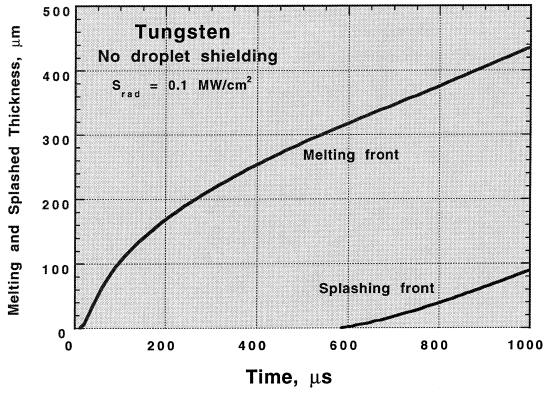

Fig. 3. Time dependence of melting and splashing fronts due to radiation power to tungsten target.

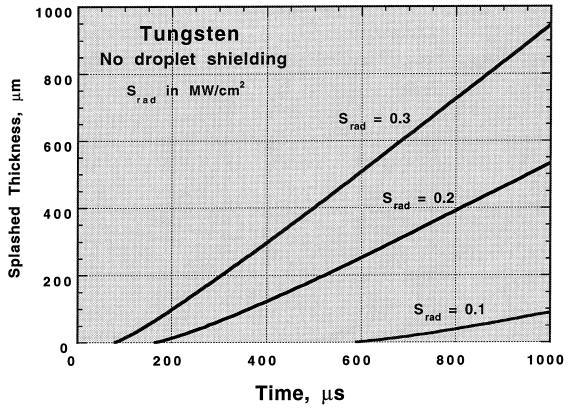

Fig. 4. Effect of net radiation power to target surface on tungsten total splashing thickness without droplet shielding.

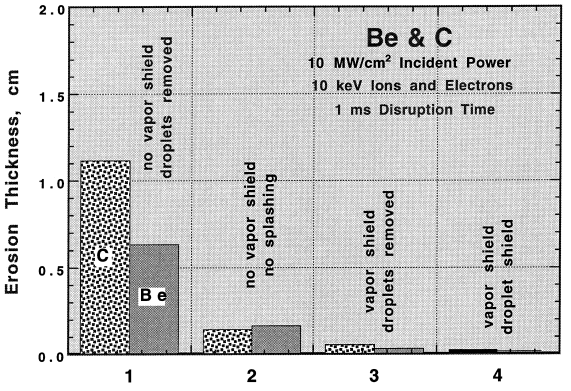

Fig. 5. Effect of vapor-cloud shielding and macroscopic particle/droplet shielding on total mass loss for Be and C during disruption.

There are four possible erosion scenarios during plasma/target interaction. Fig. 5 compares the erosion depth of both Be and graphite targets for these cases with and without both vapor shielding and droplet shielding. In case 1, i.e., absence of both shielding mechanisms (no vapor shielding, i.e., vapor is not well confined and there is no droplet shielding, so that droplets are splashed away from the incoming plasma), all incoming power will be spent in splashing erosion of the liquid surface. Erosion loss is very high, and this case may represent a disruption simulation device in which the incident plasma has a very high dynamic pressure exceeding the magnetic field pressure that is capable of blowing off the initial vapor cloud and liquid layers. Case 1 may also resemble a tokamak condition in which a strong MHD vapor turbulence develops and result in fast removal of vapor and droplets along target surface. In case 2, without vapor shielding and splashing (or ablation), all incoming power will be spent in vaporizing the target surface. This may occur if the vapor cloud is removed for any reason and the target material does not melt or splash/destruct.

In case 3, with vapor shielding but without droplet shielding (droplets are removed from incoming power), the net incoming radiation power to target surface is spent in splashing. This situation can occur on nearby components during a disruption on the divertor plate, in which the intense photon radiation from the hot vapor cloud deposits its power at locations with different orientations to the magnetic field lines; as a result, the vapor cloud is not well confined. Ablation can increase mass losses of by $\approx$4–5 times.

The fourth case is the most desirable and can be realized in a tokamak device if the vapor cloud is well confined with no MHD effects. Therefore, a well-confined vapor and droplet cloud can reduce erosion losses by up to two orders of magnitude.

5. Conclusions

Erosion of plasma-facing materials is governed by both the characteristics and distribution of incident plasma particles from the SOL, as well as by processes resulting in vapor and droplet formation and shielding. Models and theories have been developed for material erosion during intense deposition of energy on target surfaces. Most mass losses resulting from plasma/target interaction during plasma instabilities are from ablation, i.e., emission of droplets due to liquid splashing or macroscopic particles as a result of brittle destruction. Therefore, a mixture of vapor cloud and macroscopic particles exists near the target surface. Influence of such 'aerosol' on vapor cloud dynamics and the net heat load onto the target surface depends on the geometrical location of the divertor system and the existence of MHD turbulence of the vapor plasma in an oblique and strong magnetic fields. Various cases of existence or absence of vapor and droplet cloud shielding, as well as the existence of MHD instabilities, are considered and the corresponding mass losses are estimated, as are lifetimes of plasma-facing materials. The use of a renewable material such as free-surface liquid lithium may significantly extend the lifetime of PFMs and substantially enhance the tokamak concept for power-production reactors.

Acknowledgements

This work is supported by the US Department of Energy, Office of Fusion Energy, under Contract W-31-109-Eng-38.

References

[1] A. Hassanein, I. Konkashbaev, Theory and models of material erosion and lifetime during plasma instabilities in a tokamak environment, in: Presented at the Fifth International Symposium on Fusion Technology (ISFNT-5), 19–24 September 1999, Rome, Italy, Fus. Eng. Design (to be published).
[2] A. Hassanein, I. Konkashbaev, J. Nucl. Mater. 273 (1999) 326.
[3] A. Hassanein, Fus. Technol. 30 (1996) 713.
[4] A. Hassanein, I. Konkashbaev, Suppl. J. Nucl. Fus. 5 (1994) 193.
[5] V. Belan et al., J. Nucl. Mater. 233–237 (1996) 763.
[6] V. Litunovsky et al., in: B. Beaumont, P. Libeyre, B. de Gentile, G. Tonon (Eds.), Fusion Technology, 1998, p. 59.
[7] N.I. Arkhipov et al., J. Nucl. Mater. 233–237 (1996) 767.
[8] A. Hassanein, Fus. Technol. 15 (1989) 513.
[9] V. Litunovsky et al., in: 16th IEEE/NPSS Symposium on Fusion Engineering, September 30–October 5, Champaign, IL, 1995, p. 435.
[10] T. Burtseva et al., Plasma Devices Operations 4 (1995) 31.

[11] J. Linke et al., in: B. Keen, M. Huguet, R. Hemsworth (Eds.), Fusion Technology, 1991, p. 428.
[12] J. Van der laan, J. Nucl. Mater. 162–164 (1989) 964.
[13] A.V. Burdakov et al., J. Nucl. Mater. 233–237 (1996) 697.
[14] A. Hassanein, I. Konkashbaev, J. Nucl. Mater 233–237 (1996) 713.
[15] A. Hassanein et al., in: K. Herschbach, W. Maurer, J.E. Vetter (Eds.), Fusion Technology, 1994, p. 223.
[16] V. Litunovsky et al., in: Proceedings of the 20th Symposium on Fusion Technology (SOFT), 7–11 September, Marseille, France 1, 1998, p. 59.